PERFORMANCE OF A NON LINEAR DYNAMIC VIBRATION ABSORBERS

F. Djemal

Laboratory of Mechanics, Modeling and Manufacturing
National School of Engineers of Sfax
Sfax, Tunisia

Engineering Laboratory of Mechanical Systems and Materials
Higher Institute of Mechanics of Paris
Paris, France

F. Chaari

Laboratory of Mechanics, Modeling and Manufacturing
National School of Engineers of Sfax
Sfax, Tunisia

J.-L. Dion F. Renaud I. Tawfiq

Engineering Laboratory of Mechanical Systems and Materials
Higher Institute of Mechanics of Paris
Paris, France

M. Haddar

Laboratory of Mechanics, Modeling and Manufacturing
National School of Engineers of Sfax
Sfax, Tunisia

ABSTRACT

The most common method of vibration control is the use of the dynamic absorbers. Two types of absorbers can be found: Linear and nonlinear. The use of linear absorbers allows reducing vibration but only at the resonance frequency, whereas nonlinear absorbers attenuate vibration on a wide band of frequency. In this paper, a nonlinear two degrees of freedom (DOF) model is developed. A cubic nonlinearity induced by a gap is considered. The objective of the paper is to characterize nonlinear vibration of the system by applying explicit formulation (EF). An experimental study is performed to validate the numerical results. The jump phenomenon is the principal nonlinear dynamic phenomenon observed on both numerical and experimental investigations.

Keywords: Frequency response function, Nonlinear vibration absorber, Jump phenomenon.

1. INTRODUCTION

Tuned Vibration Absorber (TVA) has been invented since 1900s [1]. It is mainly composed of a mass, a spring and a damper and has a great effect in suppressing vibrations of machines and structures [2,3]. Optimal parameters were determined for the optimization of nonlinear dynamic vibration absorbers. Technical aspects were considered for its implementation [4,5].

Optimization was also carried for linear and nonlinear dynamic vibration absorbers in the case of damped primary systems. Attenuation of vibration amplitude by means of nonlinear springs was highlighted in [6-8]. Systems with nonlinear damping and nonlinear springs were studied by Zhu *et al*. [9]. They noticed that some reduction of the vibration amplitude can be obtained by adjusting the parameters of the nonlinear dampers, nonlinear spring stiffness and excitation frequency.

It has been shown that the nonlinear vibration absorber incorporating a nonlinear coupling spring element could offer performance advantages in a large frequency range [10-13]. But, unfortunately, the presence of nonlinearities may introduce dynamic instabilities and result in amplification rather than reduction of the vibration [14,15].

In this work, a two degrees of freedom (DOF) system submitted to a harmonic force is studied. It has a nonlinear behavior due to an imposed gap. To investigate the dynamics of this system, a nonlinear formulation in frequency domain is developed [16]. Dynamic responses of the linear and nonlinear systems are compared using Frequency Response Function (FRF) and nonlinear normal modes (NNM). A test rig was developed in order to validate numerical results. Analytical and experimental results are presented and discussed.

2. DYNAMIC MODEL OF THE TWO DOF SYSTEM

The investigated system is a linear oscillator (LO) attached to a nonlinear dynamic vibration absorber

* Corresponding author (fathidjemal@yahoo.fr)

DOI : 10.1017/jmech.2014.76
Copyright © 2014 The Society of Theoretical and Applied Mechanics, R.O.C.
https://doi.org/10.1017/jmech.2014.76 Published online by Cambridge University Press

(NDVA). The LO is a single mass spring model. The spring K_1 is represented by two parallel steel beams fixed in one side. The length of the two beams can be modified so that the spring stiffness can be adjusted. The vibration absorber is composed of two thin blades and a small mass M_2 embedded to the LO. Position of M_2 on the blades can be modified so that it is possible to vary the absorber stiffness. In addition, weights can be added to the absorber to modify its mass. The non linearity is due to a gap of 1mm on either side of the mass M_1 and the blades (Fig. 1).

Table 1 presents the geometric characteristics of the investigated system

The dynamic model of the investigated system consists of two masses M_1 and M_2, two linear springs K_1 and K_2 and two linear dampers C_1 and C_2. Non linearity is represented by the contact stiffness K_c. A sinusoidal force F is applied to the mass M_1 (Fig. 2).

The equations of motion of this system are given by:

$$[M]\{\ddot{X}\}+[C]\{\dot{X}\}+[K]\{X\}+\{F_c\}=\{F_{ext}\} \tag{1}$$

where $\{X\}=\{x_1,\ x_2\}^T$, $\{\dot{X}\}$ and $\{\ddot{X}\}$ represent respectively the generalized displacements, velocities and accelerations.

$[M]$ is the mass matrix of the system given by:

$$[M]=\begin{bmatrix} M_1 & 0 \\ 0 & M_2 \end{bmatrix}$$

$[C]$ is the damping matrix of the system expressed by:

$$[C]=\begin{bmatrix} C_1+C_2 & -C_2 \\ -C_2 & C_2 \end{bmatrix}$$

$[K]$ is the stiffness matrix of the system given by:

$$[K]=\begin{bmatrix} K_1+K_2 & -K_2 \\ -K_2 & K_2 \end{bmatrix}$$

$\{F_{ext}\}$ is the external forces vector applied to the system:

$$\{F_{ext}\}=\begin{Bmatrix} F \\ 0 \end{Bmatrix}$$

$\{F_c\}$ is the nonlinear force vector which is due to the contact that can occur between the two masses M_1 and M_2:

$$\{F_c\}=\begin{Bmatrix} -F_c \\ F_c \end{Bmatrix}$$

F_c is defined by the non-analytical expression as follows:

$$F_c=\begin{cases} 0 & \text{if } |\delta|<g \\ K_c(\delta-g) & \text{if } \delta>g \\ K_c(\delta+g) & \text{if } \delta<-g \end{cases} \tag{2}$$

where $2g$ is the total gap. $\delta(t)=x_1(t)-x_2(t)$ is the relative displacement between the two masses M_1 and M_2. K_c is the contact stiffness supposed to be constant.

Table 1 Geometric characteristics.

		Material	Dimensions (mm)
Linear oscillator	Mass M_1	Steel	20 × 20 × 90
	2 beams	Steel	20 × 2 × 240
absorber	Mass M_2	Steel	16 × 30 × 40
	2 blades	aluminium	20 × 0.5 × 150

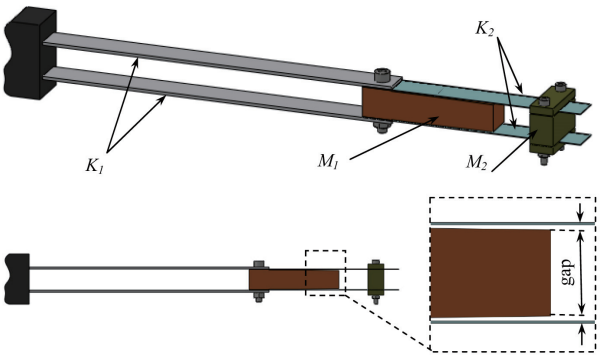


Fig. 1 Geometric model.

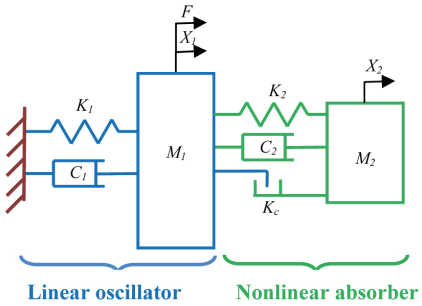


Fig. 2 Dynamic model of the investigated system.

F_c can also be written by:

$$F_c=K_c\,\tilde{h}\big(\delta(t),g\big)=K_c\begin{cases} 0 & \text{if } |\delta|<g \\ (\delta-g) & \text{if } \delta>g \\ (\delta+g) & \text{if } \delta<-g \end{cases} \tag{3}$$

The nonlinear function $\tilde{h}\big(\delta(t),g\big)$ is modeled through smoothing functions $\tilde{f}\big(\delta(t),g\big)$ as follows:

$$\tilde{h}\big(\delta(t),g\big)=\delta(t)+\frac{\tilde{f}\big(\delta(t)-g\big)-\tilde{f}\big(\delta(t)+g\big)}{2} \tag{4}$$

The smoothing function used by Kim *et al.* [17] is:

$$\tilde{f}(W)=W\tanh(\sigma W) \tag{5}$$

$$\text{With: } W=\delta(t)\pm g \tag{6}$$

σ is a coefficient reflecting the degree of nonlinearity. So, combining the two last equations yields to:

https://doi.org/10.1017/jmech.2014.76 Published online by Cambridge University Press

$$\tilde{f}\left(\delta(t)\pm g\right)=\left(\delta(t)\pm g\right)tanh\left(\sigma.\left(\delta(t)\pm g\right)\right) \quad (7)$$

The series expansion to order 3 of hyperbolic tangent function is given by the following equation:

$$\tanh(W)=W-\frac{1}{3}(W)^3+\theta(W^3) \quad (8)$$

The nonlinear function $\tilde{h}\left(\delta(t),g\right)$ can be written as follows:

$$\tilde{h}\left(\delta(t),g\right)=\left(1-2\sigma g+\frac{4}{3}\sigma^3 g^3\right)\delta(t)+\left(\frac{4}{3}\sigma^3 g\right)\left(\delta(t)\right)^3 \quad (9)$$

Equation (3) becomes:

$$F_c=K_c\,\tilde{h}\left(\delta(t),g\right)=K_c\left(1-2\sigma g+\frac{4}{3}\sigma^3 g^3\right)\delta(t)+K_c\left(\frac{4}{3}\sigma^3 g\right)\left(\delta(t)\right)^3 \quad (10)$$

Figure 3 shows the theoretical contact force presented by Eq. 3 and its approximation presented by Eq. 10.

3. NONLINEAR FORMULATION

The equation of motion of a linear undamped mass-spring system in the frequency domain and expressed in a matrix form, is:

$$[M]\left\{\ddot{X}(\omega)\right\}+[K]\left\{X(\omega)\right\}=\{F\} \quad (11)$$

$[M]$ and $[K]$ are respectively the mass and stiffness matrices. $\{F\}$ is the harmonic excitation vector operating at frequency ω.

The nonlinearity is introduced by the nonlinear contact force expressed by (10). The value of the gap is small so that:

$$1-2\sigma g+\frac{4}{3}\sigma^3 g^3\approx 1$$

The nonlinear contact force can be written as:

$$F_c=K_c\,\delta(t)+K_c\left(\frac{4}{3}\sigma^3 g\right)\left(\delta(t)\right)^3 \quad (12)$$

F_c can be expressed by the mathematical model given by the function $\tilde{g}(\tilde{x})$ as [16]:

$$\tilde{g}(\tilde{x})=k\tilde{x}+\beta\tilde{x}^3 \quad (13)$$

$$\text{With}\begin{cases}k=K_c\\ \beta=K_c\left(\frac{4}{3}\sigma^3 g\right)\end{cases}$$

$\tilde{g}(\tilde{x})$ is the force induced by an elongated spring by a distance $\tilde{x}$. The coefficient k represents the linear component of the spring and the coefficient β accounts for the nonlinear effects due to the term $\tilde{x}^3$.

By introducing (11) in (10), we obtain:

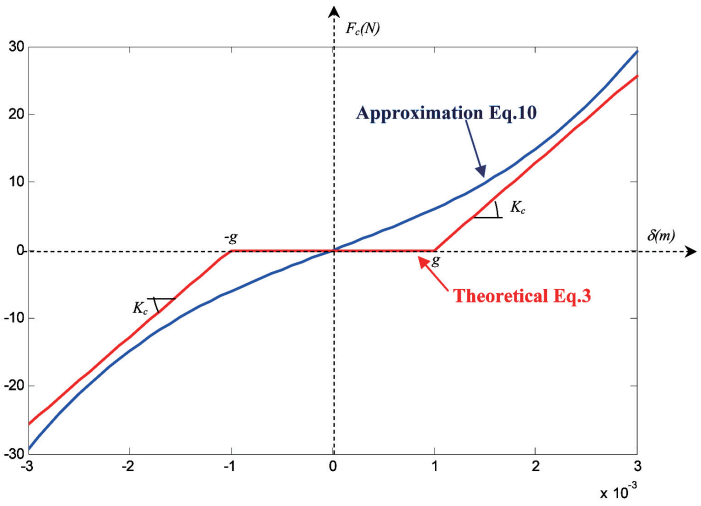


Fig. 3 Contact force.

$$[M]\left\{\ddot{\tilde{X}}(\omega)\right\}+[K]\left\{\tilde{X}(\omega)\right\}+\left\{\tilde{G}(\tilde{x}^3)\right\}=\{F\}\,e^{i\omega t} \quad (14)$$

$\{\tilde{X}\}$ is the vector of generalized coordinates of the nonlinear system.

$\left\{\tilde{G}(\tilde{x}^3)\right\}$ is a nonlinear vector defined by:

$$\left\{\tilde{G}(\tilde{x}^3)\right\}=\begin{Bmatrix}\tilde{g}_{11}+\tilde{g}_{12}+\ \dots\ +\tilde{g}_{1N}\\ \tilde{g}_{21}+\tilde{g}_{22}+\ \dots\ +\tilde{g}_{2N}\\ .\\ .\\ \tilde{g}_{N1}+\tilde{g}_{N2}+\ \dots\ +\tilde{g}_{NN}\end{Bmatrix} \quad (15)$$

Each component $\tilde{g}_{ij}$ describes the presence or not of nonlinearity between DOFs i and j. It can be expressed by:

$$\tilde{g}_{ij}(\tilde{x}_{i,j}^3)=\beta\tilde{x}_{i,j}^3 \quad (16)$$

Linearization of $\tilde{g}_{ij}$ can be done as following:

$$\tilde{g}_{ij}(\tilde{x}_{i,j}^3)=\tilde{\nu}_{ij}(\tilde{x}_{i,j}^2).\tilde{x}_{i,j} \quad (17)$$

The function $\tilde{\nu}_{ij}(\tilde{x}_{i,j}^2)$ is defined by the relation [16]:

$$\tilde{\nu}_{ij}(\tilde{x}_{i,j}^2)=\frac{1}{\pi\tilde{X}}\int_0^{2\pi}\tilde{g}_{ij}(\tilde{x}_{i,j}^3)\left[\sin(\tau)+\cos(\tau)\right]\,d\tau \quad (18)$$

In a multi degrees of freedom system $\tilde{x}_{i,j}$ represent a coupling between the degrees of freedom. For example $\tilde{x}_{1,2}$ is written by:

$$\tilde{x}_{1,2}=\tilde{x}_1-\tilde{x}_2 \quad (19)$$

In the general case, the function is obtained by:

https://doi.org/10.1017/jmech.2014.76 Published online by Cambridge University Press

$$\tilde{g}_{ij}(\tilde{x}^3_{i,j}) = \left[\frac{3}{4}\beta_{ij} \mid \tilde{X}_{i,j} \mid^2 \quad -\frac{3}{4}\beta_{ij} \mid \tilde{X}_{i,j} \mid^2\right]\begin{Bmatrix}\tilde{X}_i \\ \tilde{X}_j\end{Bmatrix} \tag{20}$$

Rearranging Eq. (14) yields to:

$$\left(-\omega^2[M]+[K]+\left[\tilde{\nu}(\tilde{x}^2_{i,j})\right]\right)\left\{\tilde{X}(\omega)\right\} = \{F\} \tag{21}$$

The resolution of this set of equations is accomplished using the Newton-Raphson method. The nonlinear eigenvalue problem to be solved is:

$$\left(-\omega^2[M]+[K]\right)[\tilde{\Phi}]\{\tilde{P}\}+\left\{\tilde{G}(\tilde{x}_{i,j})\right\} = 0 \tag{22}$$

$[\tilde{\Phi}]$ is the nonlinear eigenvectors matrix depending on the amplitude and frequency. This matrix can be decomposed into two matrices and we can write:

$$[\tilde{\Phi}] = [\Phi + \Delta\tilde{\Phi}] \tag{23}$$

where Φ is the eigenvectors matrix, $\Delta\Phi$ is the nonlinear variation of the eigenvectors.

By analogy with the linear case, we can write:

$$\begin{aligned}&\{\tilde{P}\} = \tilde{\Phi}^{-1}\{\tilde{X}\}\\ &[\tilde{\lambda}^2 - \omega^2]\{\tilde{P}\} = [\tilde{\Phi}]^T\{F\}\\ &[\Phi]^T[K][\Phi] = [\lambda^2]\end{aligned} \tag{24}$$

The system response can be obtained by solving Eq. (22):

$$\{\tilde{X}\} = \frac{[\tilde{\Phi}][\tilde{\Phi}]^T\{F\}}{[\tilde{\lambda}^2 - \omega^2]} \tag{25}$$

where $\tilde{\lambda}$ are the nonlinear eigenvalues. They are defined by:

$$\tilde{\lambda}^2 = \lambda^2 + \Delta\tilde{\lambda}^2 \tag{26}$$

For each mode r, the variation $\Delta\tilde{\lambda}_r$ is defined by:

$$\Delta\tilde{\lambda}^2_r = \frac{(\Phi^T\tilde{G})_r + \left((\lambda^2-\omega^2)\,\Phi^{-1}\Delta\tilde{\Phi}\{\tilde{P}\}\right)_r + (\Delta\tilde{\Phi}^T F)_r}{\{\tilde{P}\}_r} \tag{27}$$

For mode s, the ratio of the i^{th} component of the nonlinear solution vector to the j^{th} component of the external force vector is defined by:

$$\frac{\tilde{X}_i}{F_j} = \frac{\tilde{\phi}_{is}\,\tilde{\phi}_{js}}{\tilde{\lambda}^2_s - \omega^2} + \sum_{\substack{r=1\\ r\neq s}}^{L}\frac{\phi_{ir}\,\phi_{jr}}{\tilde{\lambda}^2_r - \omega^2} \tag{28}$$

The computation procedure of nonlinear modes is shown by the following chart (Fig. 4).

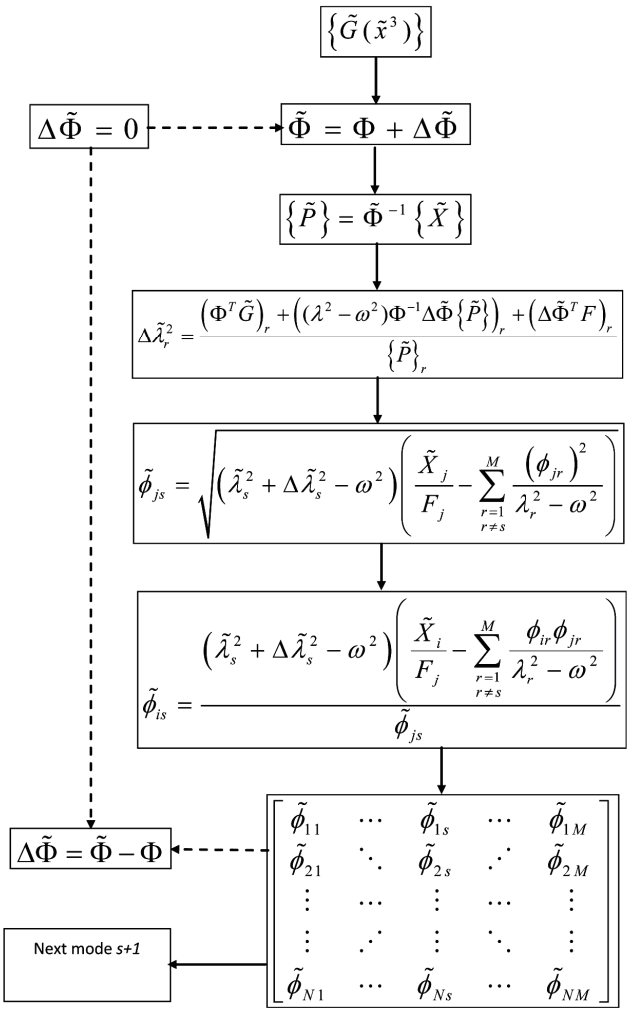


Fig. 4 Chart of the nonlinear modal computation.

4. NUMERICAL SIMULATION

The investigated system has a linear behavior in the case of low force amplitude since there is no contact between the blades and the Mass M_1.

Table 2 presents the parameters of the studied system:

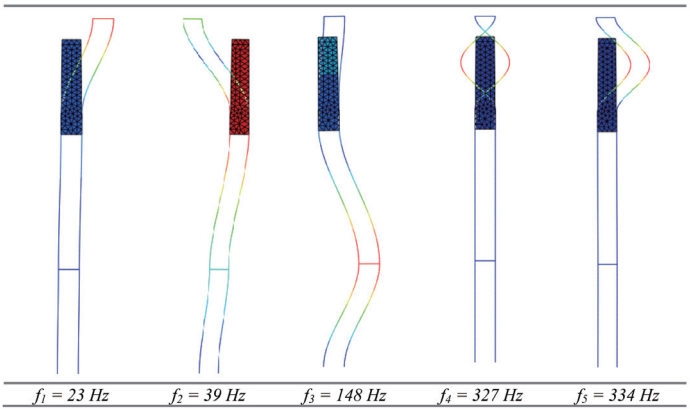
Table 2 Mechanical properties.

Parameters	Value
Mass M_1 (kg)	0.36
mass M_2 (kg)	0.09
Stiffness K_1(N/m)	12800
Stiffness K_2 (N/m)	3000
Damping C_1(N/m.s^{-1})	1.3
Damping C_2(N/m.s^{-1})	0.3

A frequency analysis is performed by the finite element software ABAQUS. Table 3 shows the first five natural frequencies of the system.

https://doi.org/10.1017/jmech.2014.76 Published online by Cambridge University Press

Table 3 First five natural frequencies an corresponding mode shapes.



The two first natural frequencies are $f_1 = 23$Hz and $f_2 = 39$Hz. We will consider the frequency range of excitation covering only these two natural frequencies. Knowing also the values of the masses M_1 and M_2, it is possible to estimate the values of stiffness K_1 and K_2 by solving the analytical formula of natural frequencies for a 2 DOF system given by:

$$\begin{cases} \omega_1^2 = \dfrac{1}{2}\left(\left(\dfrac{K_1+K_2}{M_1}\right)^2 + \left(\dfrac{K_2}{M_2}\right)^2\right) \\ -\dfrac{1}{2}\left[\left(\left(\dfrac{K_1+K_2}{M_1}\right)^2 - \left(\dfrac{K_2}{M_2}\right)^2\right)^2 + 4\,\dfrac{K_2^2}{M_1M_2}\right]^{1/2} \\ \omega_2^2 = \dfrac{1}{2}\left(\left(\dfrac{K_1+K_2}{M_1}\right)^2 + \left(\dfrac{K_2}{M_2}\right)^2\right) \\ +\dfrac{1}{2}\left[\left(\left(\dfrac{K_1+K_2}{M_1}\right)^2 - \left(\dfrac{K_2}{M_2}\right)^2\right)^2 + 4\,\dfrac{K_2^2}{M_1M_2}\right]^{1/2} \end{cases} \tag{29}$$

The eigenvalues and eigenvectors are defined by:

$$\lambda^2 = \begin{bmatrix} \omega_1^2 & 0 \\ 0 & \omega_2^2 \end{bmatrix} = \begin{bmatrix} 21129 & 0 \\ 0 & 56093 \end{bmatrix},$$
$$\Phi = \begin{bmatrix} \Phi_{11} & \Phi_{12} \\ \Phi_{21} & \Phi_{22} \end{bmatrix} = \begin{bmatrix} -0.9847 & -1.3447 \\ -2.6894 & 1.9694 \end{bmatrix}$$

The damping is chosen to be proportional to mass and stiffness matrices [18].

$$C = a\,M + b\,K (a = 0.05 \text{ and } b = 10^{-4})$$

Figure 5 shows the linear frequency response for each degree of freedom X_1 and X_2 (X_1 refers to the LO and X_2 refers to the absorber). Each response shows two resonance peaks corresponding to the linear natural frequencies of the system.

In the case of high force amplitude and for certain excitation frequencies the two thin blades reach to tape on the mass M_1so that the investigated system has a nonlinear behavior. The nonlinearity in stiffness can be defined by the following function:

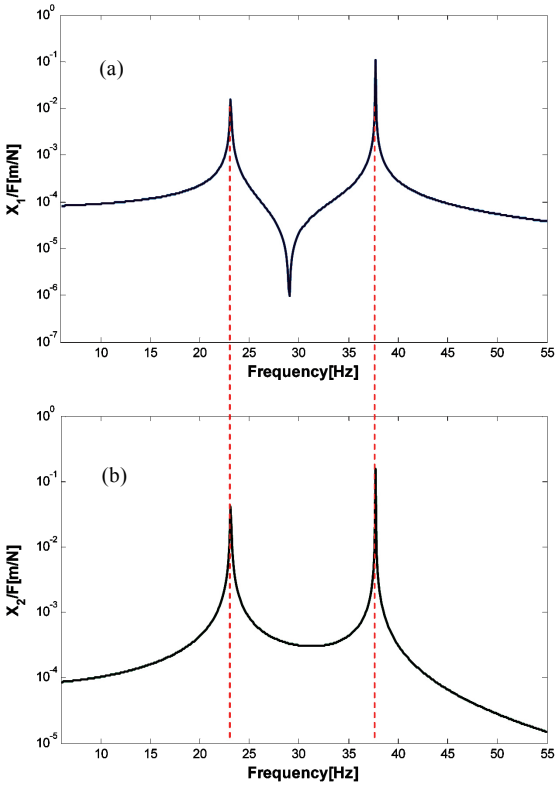


Fig. 5 FRF of the linear system: (a) LO, (b) absorber.

$$\begin{aligned} \tilde{g}_{12}(\tilde{x}_{1,2}) &= \beta_{12}(\tilde{x}_1 - \tilde{x}_2)^3 \\ \tilde{g}_{21}(\tilde{x}_{2,1}) &= \beta_{21}(\tilde{x}_2 - \tilde{x}_1)^3 \end{aligned} \tag{30}$$

The dynamic behaviour of the nonlinear system is described in the form:

$$[M]\ddot{\tilde{X}} + [K]\tilde{X} + \tilde{G}(\tilde{x}^3) = Fe^{i\omega t} \tag{31}$$

The vector $\tilde{G}(\tilde{x}^3)$ is defined as:

$$\tilde{G}(\tilde{x}^3) = \begin{Bmatrix} \tilde{g}_{12}(\tilde{x}_{1,2}) \\ \tilde{g}_{21}(\tilde{x}_{2,1}) \end{Bmatrix} \tag{32}$$

with

$$\begin{aligned} \tilde{g}_{12}(\tilde{x}_{1,2}) &= \begin{bmatrix} \frac{3}{4}\beta_{12} \mid \tilde{X}_1 - \tilde{X}_2 \mid^2 & -\frac{3}{4}\beta_{12} \mid \tilde{X}_1 - \tilde{X}_2 \mid^2 \end{bmatrix} \begin{Bmatrix} \tilde{X}_1 \\ \tilde{X}_2 \end{Bmatrix} \\ \tilde{g}_{21}(\tilde{x}_{2,1}) &= \begin{bmatrix} \frac{3}{4}\beta_{21} \mid \tilde{X}_2 - \tilde{X}_1 \mid^2 & -\frac{3}{4}\beta_{21} \mid \tilde{X}_2 - \tilde{X}_1 \mid^2 \end{bmatrix} \begin{Bmatrix} \tilde{X}_1 \\ \tilde{X}_1 \end{Bmatrix} \end{aligned} \tag{33}$$

Equation (29) becomes:

$$[M]\ddot{\tilde{X}} + [K]\tilde{X} + \left[\tilde{v}(\tilde{x}^2)\right]\tilde{X} = Fe^{i\omega t} \tag{34}$$

where $\left[\tilde{v}(\tilde{x}^2)\right]$ is defined as:

https://doi.org/10.1017/jmech.2014.76 Published online by Cambridge University Press

$$\left[\tilde{v}(\tilde{x}^2)\right]=\frac{3}{4}\begin{bmatrix}\beta_{12}\mid\tilde{X}_1-\tilde{X}_2\mid^2 & -\beta_{12}\mid\tilde{X}_1-\tilde{X}_2\mid^2\\ -\beta_{21}\mid\tilde{X}_2-\tilde{X}_1\mid^2 & \beta_{21}\mid\tilde{X}_2-\tilde{X}_1\mid^2\end{bmatrix} \quad (35)$$

The nonlinearity is introduced into the model by the constant $\beta_{12}=\beta_{21}=1.28\times10^6$.

Figure 6 presents a comparison between the linear response characterised by the presence of peaks corresponding to the two resonance frequencies and the nonlinear response characterized by the jump phenomenon (discontinuity of responses). This jump is close to the two linear natural frequencies of the system for the primary mass (LO) and the absorber.

We note that the amplitudes of the frequency response near the natural frequencies are significantly attenuated.

Figure 7 shows the discontinuities of the eigen values in the vicinity of the two natural frequencies of the system. These discontinuities are caused by nonlinearity introduced by the cubic stiffness model.

Figure 8 shows the discontinuity of the components of the nonlinear modal matrix depending on the excitation force frequency ω. This discontinuity is always in the vicinity of the natural frequencies of the model.

For the two modes it is clear that the modal deflections are, as for the LO, in phase for the first mode and counterphased for the second one.

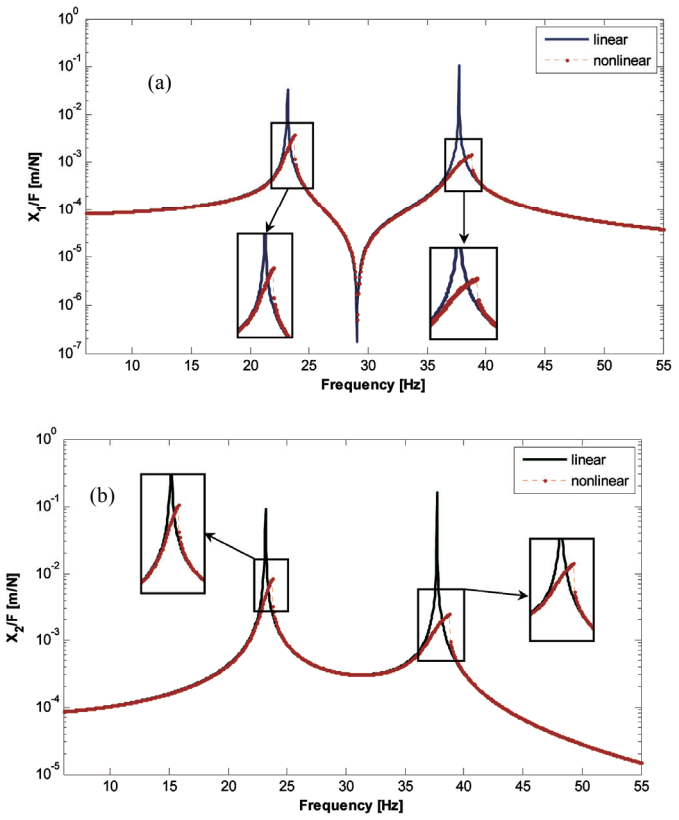


Fig. 6 FRF of the nonlinear system: (a) LO, (b) absorber.

5. EXPERIMENTAL RESULTS AND DISCUSSION

In this section, an experimental study is performed to validate the numerical results. As shown in Fig. 9, the main system is directly connected to an electrodynamic shaker and is subjected to a harmonic force. The electrodynamic shaker is excited by a signal generator producing a stepped-sine signal. The exciting force is measured by a load cell. The accelerations of the two masses are measured using piezoelectric sensors. Measurements are directed to National Instruments NI-PXI 4462 data acquisition card and processed by Labview software.

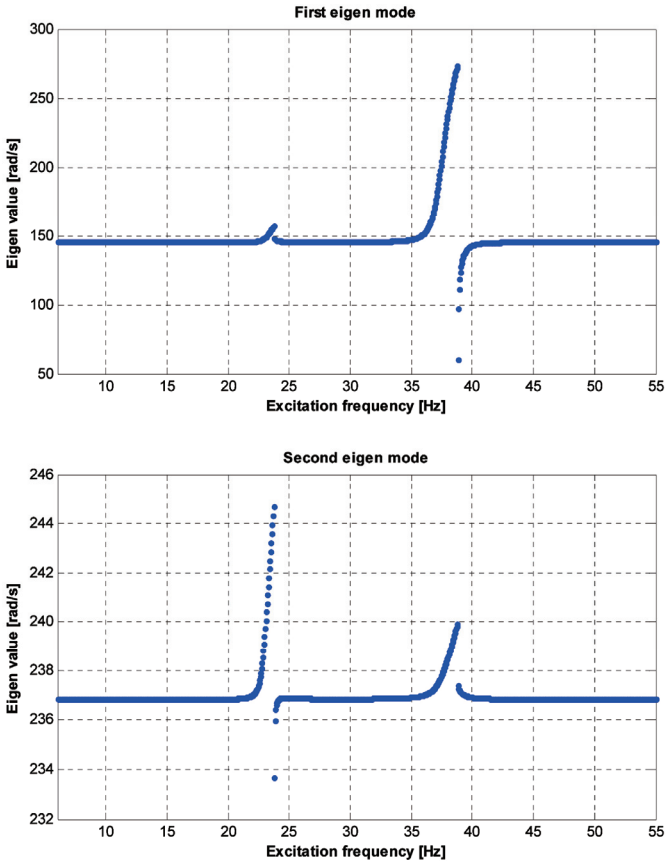


Fig. 7 Discontinuity of the nonlinear normal mode.

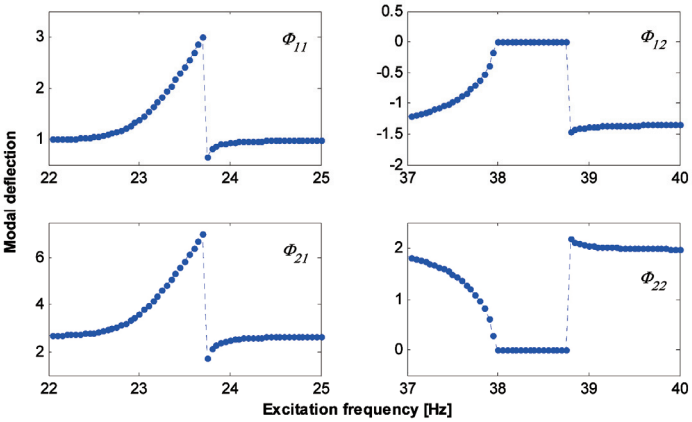


Fig. 8 Discontinuity of the vector components of the nonlinear modal matrix.

https://doi.org/10.1017/jmech.2014.76 Published online by Cambridge University Press

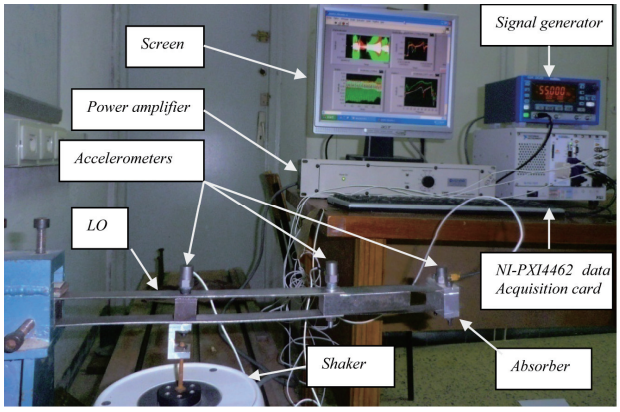


Fig. 9 Experimental setup.

The schematic diagram of the experimental setup is shown in Fig. 10.

A preliminary test consists of a frequency sweep to determine the resonant frequencies and the frequency band set to be studied. The length of the beams and the position of the absorber mass are well adjusted to limit the frequency band sweep. For each test, different force amplitudes are applied by the shaker and measured by a load cell. A slow frequency sweep was applied from 6Hz to 55Hz and the response of the system was recorded via the data acquisition card. The sweep frequency is performed in increasing and decreasing ways. The variation of the frequency was done at a very slow rate such that the registered results can be safely considered to represent the steady-state behavior of the system.

Figure 11 shows the time measurement of acceleration in the case of increasing and decreasing frequency for the two masses M_1 an M_2. The sweep rate during increasing and decreasing frequency is of 100 seconds.

We start with low excitation force amplitude. There is no contact between the absorber and the LO so that the system present linear behavior. Two resonant frequencies are observed with large vibrational amplitudes in both masses.

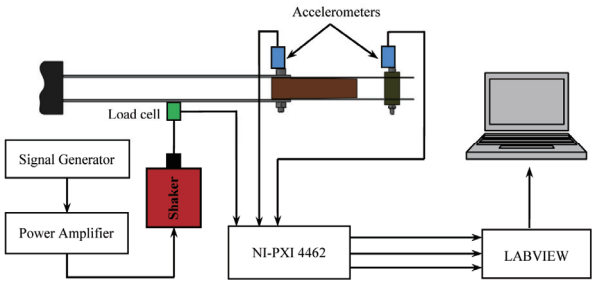
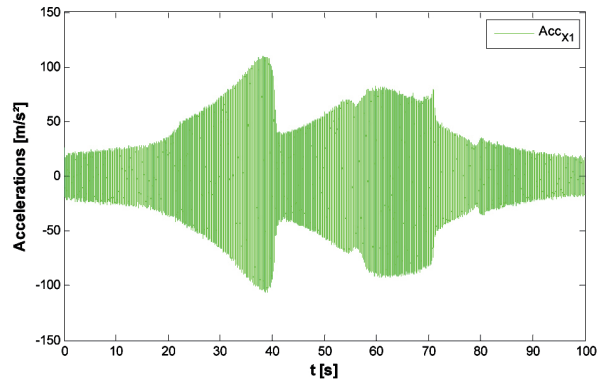
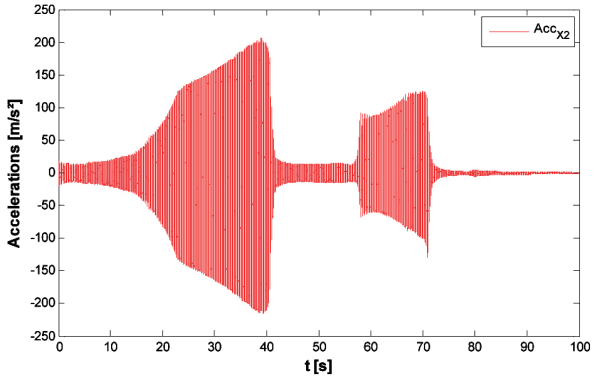
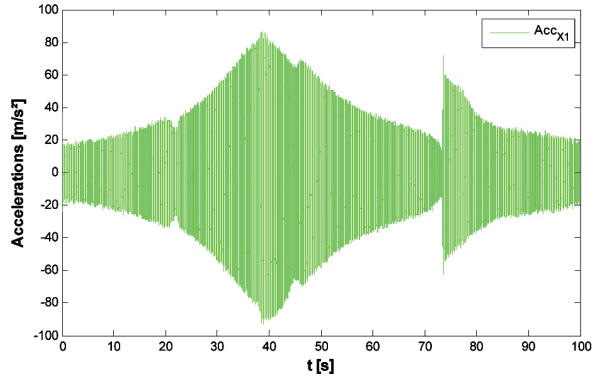


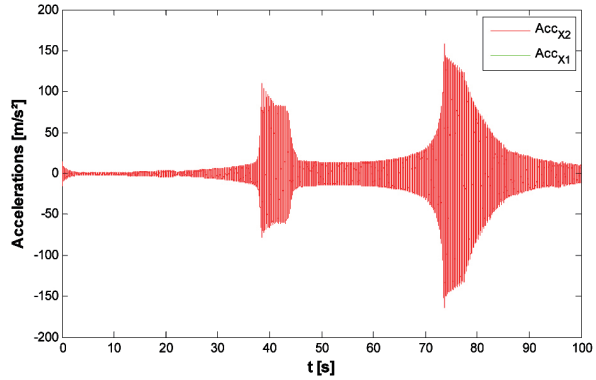
Fig. 10 Schematic diagram of the instrumentation setup.





(a) Increasing frequency





(b) Decreasing frequency

Fig. 11 Registered accelerations: —— (M_1), —— (M_2).

In the case of high excitation force, the two blades of the absorber reach to tape on the mass M_1. By increasing frequency, the vibration level of the two masses is increasing until reaching 25Hz. At this frequency, a sudden decrease in the amplitude of vibration of the two masses is occurred: A jump-down in the response.

https://doi.org/10.1017/jmech.2014.76 Published online by Cambridge University Press

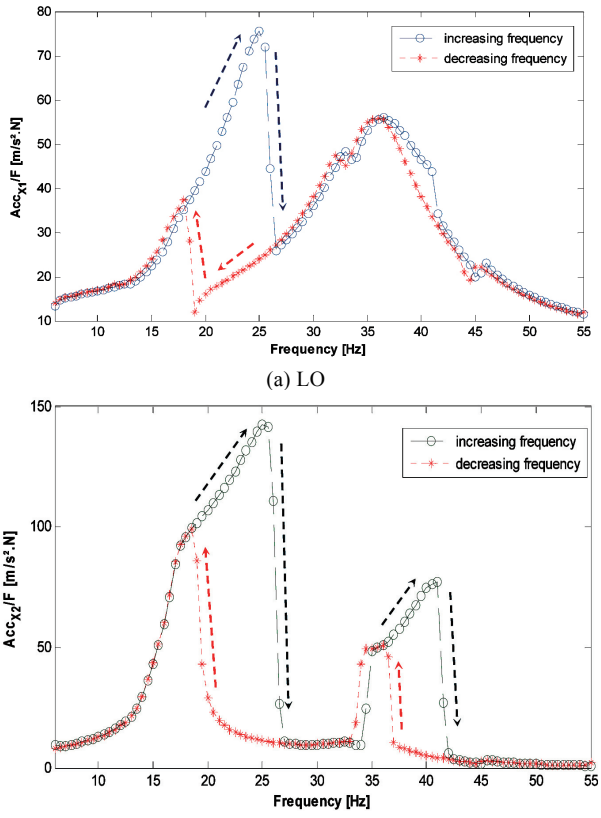
When the frequency was increased beyond this, the vibration amplitude stay insignificant. By increasing frequency again, a second resonance occurred at about 41Hz. The jump-down phenomenon is observed again especially for the absorber mass.

The frequency was then slowly swept down from this high frequency back to the low frequency (from 55Hz to 6Hz). For the mass M_1, the vibration amplitude increase practically like in the case of increasing frequency. For the mass M_2, a sudden increase in the amplitude is occurred at 36Hz (a jump-up). By decreasing frequency again, the jump-up phenomenon is occurred for the masses at about 20Hz.

Figure 12 presents the experimental frequency response of accelerations of the masses M_1 and M_2. The jump-down phenomenon occurs at around 25Hz and 41Hz. The jump-up phenomenon occurs at around 20Hz and 36Hz. The vibration amplitudes are significantly attenuated near the natural frequencies of the system.

A comparison between experimental and numerical frequency response for the two masses is shown in Fig. 13. It is well noticed a qualitative agreement in results even if there is a difference on the amplitude at jump-down and jump-up frequencies. This is due to the difficulties on the exact characterization of the nonlinear stiffness and damping.

Figure 14(a) ~ 14(b) shows the harmonics for the two masses M_1 and M_2 dynamic response which proof the presence of non linearity for the experimental device. This nonlinearity makes this system robust and with a great importance in vibration mitigation.



(a) LO

(b) Absorber

Fig. 12 Experiment frequency response of accelerations: (a) LO, (b) absorber (o) increasing frequency, (*) decreasing frequency.

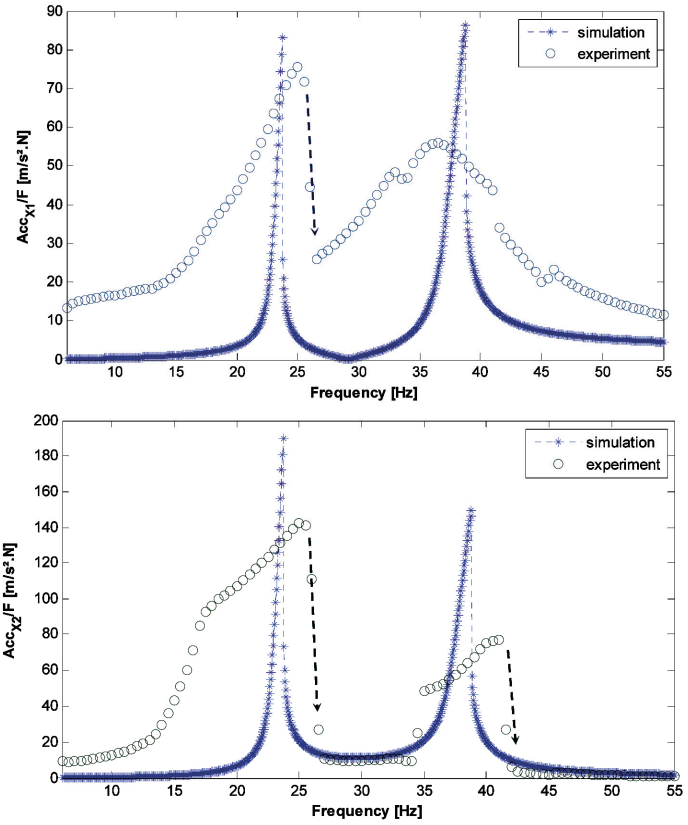


Fig. 13 Numerical and experimental frequency response: (a) LO, (b) absorber (*) simulation, (o) experiment.

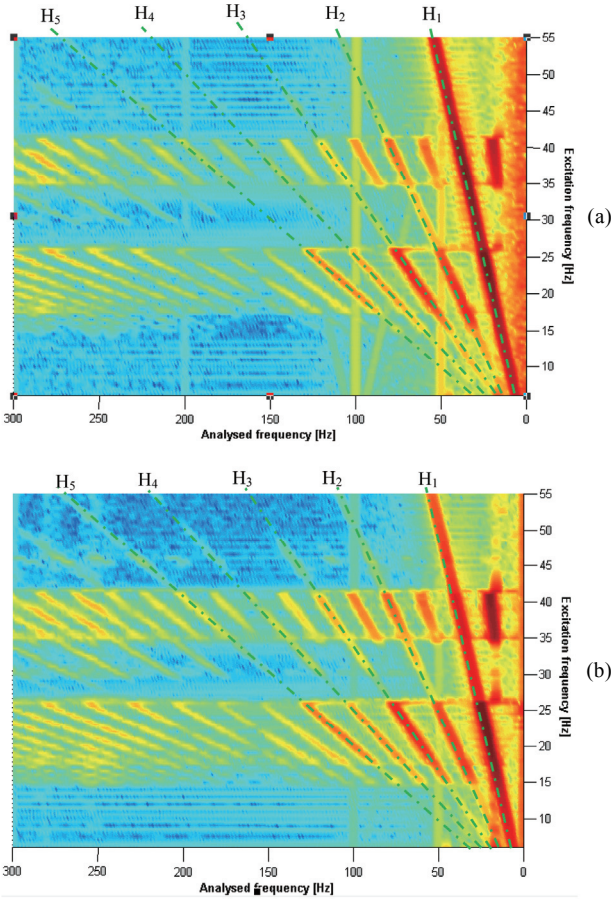


Fig. 14 harmonics of experimental response on: (a) M_1, (b) M_2.

https://doi.org/10.1017/jmech.2014.76 Published online by Cambridge University Press

6. CONCLUSIONS

In this works, an explicit formulation method to investigate the nonlinear dynamics of a two DOF system with a nonlinear cubic stiffness is investigated. The results showed that the natural frequencies of the system vary with the excitation frequency. It is also observed the existence of the jump phenomenon which characterizes the nonlinear behavior of the system. Experimental results agree with numerical simulation and illustrate the importance of the nonlinear vibration absorber in reducing the amplitude levels especially close to the natural frequencies.

REFERENCES

1. Frahm, H., "Device for Damped Vibrations of Bodies," U.S. Patent No. 989958, Washington, DC: U.S. Patent and Trademark Office (1909).
2. Ormondroyd, J. and DenHartog, J. P., "The Theory of the Dynamic Vibration Absorber," *Transactions of ASME*, **49**, pp. A9–A22 (1928).
3. Hunt, J. B., *Dynamic Vibration Absorbers*, Mechanical Engineering Publications, London, England (1979).
4. Hunt, J. B. and Nissen, J. C., "The Broad Band Dynamic Vibration Absorber," *Journal of Sound and Vibration*, **83**, pp. 573–578 (1982).
5. Nissen, J. C., Popp, K. and Schmalhorst, B., "Optimization of a Non-Linear Dynamic Vibration Absorber," *Journal of Sound and Vibration*, **99**, pp. 149–154 (1985).
6. Jordanov, I. N. and Cheshankov, B. I., "Optimal Design of Linear and Nonlinear Dynamic Vibration Absorbers," *Journal of Sound and Vibration*, **123**, pp. 157–170 (1988).
7. Soom, A. and Lee, M., "Optimal Design of Linear and Non-Linear Vibration Absorbers for Damped Systems," *Journal of Vibration, Acoustics, Stress, and Reliability in Design*, **105**, pp. 112–119 (1983).
8. Liu, K. F. and Liu, J., "The Damped Dynamic Vibration Absorbers: Revisited and New Result," *Journal of Sound and Vibration*, **284**, pp. 1181–1189 (2005).
9. Zhu, S. J., Zheng, Y. F. and Fu Y. M., "Analysis of Nonlinear Dynamics of a Two-Degree-Of-Freedom Vibration System with Non-Linear Damping and Nonlinear Spring," *Journal of Sound and Vibration*, **271**, pp. 15–24 (2004).
10. Hunt, J. B. and Nissen, J. C., "The Broad Band Dynamic Vibration Absorber," *Journal of Sound and Vibration*, **83**, pp. 573–578 (1982).
11. Nissen, J. C., Popp, K. and Schmalhorst, B., "Optimization of a Non Linear Dynamic Vibration Absorber," *Journal of Sound and Vibration*, **99**, pp. 149–154 (1985).
12. Rice, H. J. and McCraith, J. R., "On Practical Implementations of the Nonlinear Vibration Absorber," *Journal of Sound and Vibration*, **110**, pp. 161–163 (1986).
13. Bert, C. W., Egle, D. M. and Wilkins, D. J., "Optimal Design of a Nonlinear Dynamic Absorber," *Journal of Sound and Vibration*, **137**, pp. 347–352 (1990).
14. Rice, H. J., "Combinational Instability of the Non-Linear Vibration Absorber," *Journal of Sound and Vibration*, **108**, pp. 526–532 (1986).
15. Natsiavas, S., "Steady State Oscillations and Stability of Non-Linear Dynamic Vibration Absorbers," *Journal of Sound and Vibration*, **156**, pp. 227–245 (1992).
16. Siller, H. R. E., "Nonlinear modal analysis methods for engineering structures," Ph.D. Dissertation, Department of Mechanical Engineering, Imperial College London / University of London, U. K. (2004).
17. Kim T. C., Rook T. E. and Singh R., "Effect of Smoothening Functions on the Frequency Response of an Oscillator with Clearance Non-Linearity," *Journal of Sound and Vibration*, **263**, pp. 665–678 (2003).
18. Meirovitch, L., *Fundamentals of Vibrations*, McGraw-Hill, New York, U. S. (2001).

(Manuscript received February 15, 2014,
accepted for publication June 10, 2014.)

https://doi.org/10.1017/jmech.2014.76 Published online by Cambridge University Press